Optimization analysis of solid oxide fuel cells with ceria-based single cells using computational fluid dynamics

Tan Kang Huai [1*], *Mohammad Saifulddin* Mohd Azami [2], *Hamimah* Abd. Rahman[3], *Nurul Farhana* Abd Rahman[3], *Mohd Faizal* Tukimon[3], *Zol Hafizi* Jaidi[3], and *Umira Asyikin* Yusop[3]

[1]Centre for Advanced Materials, Faculty of Engineering and Technology, Tunku Abdul Rahman University of Management and Technology, Jalan Genting Kelang, 53300, Kuala Lumpur, Malaysia.
[2]Faculty of Applied Sciences, University Teknologi MARA Perlis Branch, 02600, Arau, Perlis, Malaysia.
[3]Faculty of Mechanical and Manufacturing Engineering, Universiti Tun Hussein Onn Malaysia, 86400 Parit Raja, Batu Pahat, Johor, Malaysia

Abstract. The SOFC simulations in this research are conducted at temperatures of 600°C, 700°C, and 800°C, focusing on the Ni-SDC anode, SDC electrolyte, and LSCF-SDC materials used in the SOFC single cell. Initially, the single-cell model is created using CAD software, followed by the development of a computational fluid dynamics (CFD) model with the requisite material properties. The study then proceeds to simulate temperature distribution and cell performance for various supported SOFC stack models (electrode and electrolyte supported) at intermediate temperatures. Subsequently, the study examines cell performance with varying thicknesses of the anode, electrolyte, and cathode components within the specific supported single cell. In summary, the CFD results indicate that cathode-supported SOFCs exhibit higher power density, specifically 938.28 mW/cm^2 at 800°C, surpassing anode-supported and electrolyte-supported configurations. The power density reaches 1495.40 mW/cm^2 when the single-cell layer thickness is 0.35 mm for the cathode, 0.02 mm for the anode, and 0.01 mm for the electrolyte. However, electrolyte-supported single cells display the lowest temperature difference, at 0.028% at 800ºC The simulation results demonstrate that reducing the thicknesses of all electrodes and the electrolyte leads to increased current density, power density, and temperature distribution difference.

1 Introduction

Use Solid oxide fuel cells (SOFCs) offer significant advantages, primarily when operating at elevated temperatures. High-temperature SOFCs, or HT-SOFCs, typically utilize yttria-stabilized zirconia (YSZ) composite materials, employing nickel oxide – yttria-stabilized zirconia (NiO-YSZ) as the anode and lanthanum strontium manganite – yttria-stabilized zirconia (LSM-YSZ) as the cathode. Nevertheless, SOFCs operating at such high temperatures face various degradation mechanisms, necessitating a thorough examination of their thermal behavior and durability [1][2]. However, reducing the temperature operation has enabled different material-based SOFC to be discovered and investigated. In this study, a single ceria-based cell composed of an LSCF-SDC cathode, NiO-SDC anode, and SDC electrolyte, as well as an interconnect, is incorporated to investigate thermal behavior and electrochemical performance from 600 to 800ºC.

The study of fluid flow using numerical solution methods is referred to as computational fluid dynamics (CFD). CFD enables the analysis of complex problems involving interactions between fluids, fluids and solids, and fluids and gases. Consequently, CFD has become a highly valuable and widely used tool for researchers studying transport and electrochemical phenomena within fuel cells. In contrast to experimental approaches, which often involve complex and expensive setups for analyzing SOFC performance, computational fluid dynamics (CFD) plays a central role in this project [3]. It allows for the examination of how fuel cell behavior, design performance, and various parameters are affected under diverse operating conditions. Specialized software such as ANSYS Fluent will be employed to evaluate its influence on SOFC performance.

One significant factor contributing to the reduced thermal durability of SOFCs is the generation of thermal stress [4]. These stresses result from temperature gradients among different components. Therefore, it is essential to study the temperature distribution along the single cell to investigate the maximum and minimum temperature ranges. These substantial thermal fluctuations often lead to cracking and spallation [5]. Previous studies have shown that the design of single cells, including anode-supported, cathode-supported, or electrolyte-supported cells, significantly influences thermal behavior in modeling analyses.Additionally, anode, electrolyte, and cathode materials possess distinct properties. Chelmehsara and Mahmoudimehr utilized Ni-YSZ as the anode, YSZ as the electrolyte, and LSM-YSZ as the cathode for their CFD modeling

* Corresponding author: tankanghuai@tarc.edu.my /tankanghuai@gmail.com

[6]. They reported that while the different supported SOFC exhibited the different power density with various layer thicknesses. Hence, it is crucial to determine whether cathode-supported, anode-supported, or electrolyte-supported configurations are suitable for the ceria-based single-cell model.

Furthermore, it is imperative to investigate the effects of electrode and electrolyte thickness.Several studies have explored the effects of electrolyte thickness, revealing that reducing it leads to increased maximum power density [7-9], especially at higher current densities under constant temperature conditions. However, research on the influence of electrode thickness on SOFCs remains limited. The selected thickness of the anode, cathode, and electrolyte plays a pivotal role in modeling and significantly impacts the thermal behavior and power performance of the SOFC. The results from Yang indicate that the maximum power density for anode thicknesses of 400, 600, 800, and 1000 µm is approximately 1.11, 1.07, 0.98, and 0.93 W/cm^2, respectively [10], while the study demonstrates that the maximum power density for electrolyte thicknesses of 10, 20, 30, and 40 µm is around 1.1, 0.82, 0.7, and 0.6 W/cm^2. In a study by Naseff et al., the resulting optimal cell parameters are 0.5 mm, 20 µm, and 62.26 µm for anode thickness, electrolyte thickness, and cathode thickness respectively[11]. The cell maximum power density is 1.8 W/cm^2, 2.25 W/cm^2 and 2.72 W/cm^2. Despite commendable electrochemical performance in experimental tests for individual anodes, cathodes, and electrolytes, their thickness can significantly impact overall SOFC performance.

2 Methodology

The A three-dimensional model of an SOFC stack was crafted using Autodesk Inventor software. This model encompasses three distinct designs: anode-supported, electrolyte-supported, and cathode-supported SOFCs, as visually depicted in the accompanying Figure 1. In an exampel of SOFC stack model, the supported electrode exhibits a thickness of 0.35mm, while the electrolyte and adjacent components maintain a consistent thickness of 0.02mm and 0.03mm, respectively. Moreover, the interconnect sandwiches the single cell.

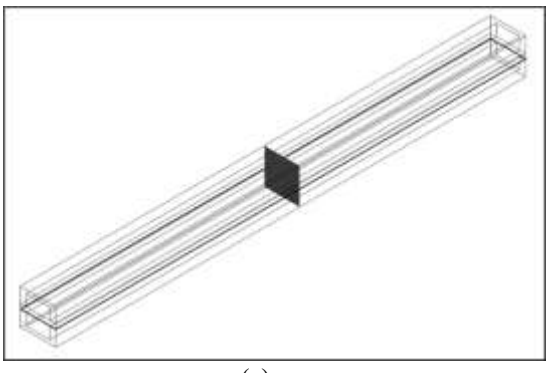

(a)

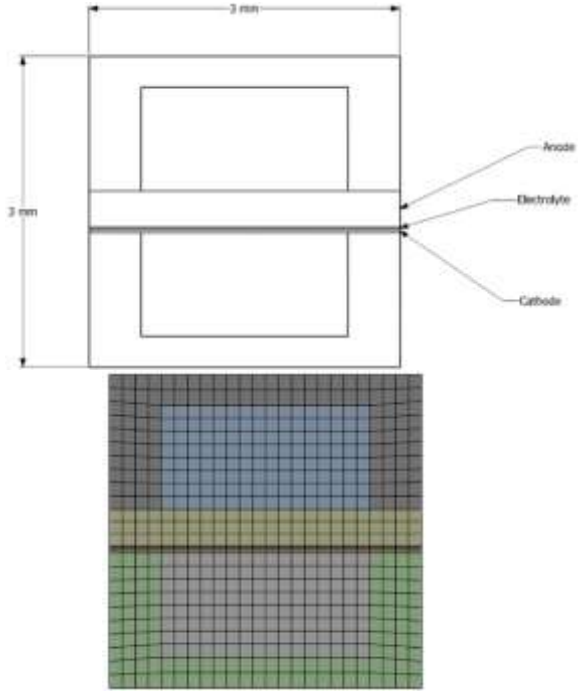

(b)

Fig.1. Schematic of SOFC Model (a) isometric view (b) cross section view of SOFC and geometry mesh

Table 1. Material Properties of SOFC components [12-15]

Material	Anode (NiO-SDC)	Electrolyte (SDC)	Cathode (LSCF-SDC)	Interconnect (SUS430)
Porosity, ε (%)	30	$1x10^{-20}$	30	-
Permeability, β (m^2)	$1x\ 10^{-12}$	$1x10^{-18}$	$1x\ 10^{-12}$	-
Electrical conductivity, σ (Ωm^{-1})	80000	-	8400	$1x10^{-16}$
Thermal conductivity, k (W/m.K)	12	2	2.7	15
Thermal expansion coefficient, TEC (× 10^{-6} K^{-1})	12.6-13.5	12.1	14.8	12
Tortuosity factor, τ	3	3	3	-

Table 2. Operating And Boundary Conditions Of SOFC Model [11]

Parameter	Value/Data
Flow Pattern	Parallel flow (Co-flow)
Inlet gas flow rate at anode side (kg/s)	1×10^{-8}
Inlet gas flow rate at cathode side (kg/s)	8×10^{-6}
Operating temperature (°C)	600 / 700 / 800
Inlet gas composition at anode side (mole fraction)	$97\%H_2 + 3\%H_2O$
Inlet gas composition at cathode side (mole fraction)	$21\%O_2 + 79\%N_2$
Operating pressure (atm)	1
Operating voltage (V)	0.7

The ANSYS Fluent solver employs the finite volume method to solve the conservation equations, utilizing elements as control volumes within the flow field. For the meshing configuration, an element size of 0.000125mm was specified, resulting in a total of 224,700 nodes and 207,360 elements within the geometric model. This element size at 0.000125mm demonstrates a high-quality mesh. The cross section of SOFC as shown in Figure 1 (b) is analysed as detail colour profile can be observed.

3 Result and discussion

First and foremost, by examining Figures 2, 3, and 4, it becomes evident that the temperature distribution within the SOFC single cell becomes more uniform as the operating temperature increases. This phenomenon can be attributed to the higher operating temperature of the SOFC, which enhances ionic conductivity, consequently promoting a more even temperature distribution [16]. Additionally, it's worth noting that the temperature distribution for all supported cell at all operating temperarure within the anode area of the single cell SOFC is generally larger than that of the electrolyte and cathode components. This disparity is primarily due to the anode component's higher thermal conductivity. When assessing the maximum and minimum temperatures at an operating temperature of 800°C, the percentage differences in temperature for the anode-supported SOFC, electrolyte-supported SOFC, and cathode-supported SOFC are approximately 0.0287%, 0.0288%, and 0.04%, respectively. Moreover, at an operating temperature of 700°C, the temperature differences percentage for these three types of SOFCs are approximately 0.0447%, 0.0381%, and 0.0724%, respectively. Lastly, at an operating temperature of 600°C, the temperature differences percentage for the anode-supported SOFC, electrolyte-supported SOFC, and cathode-supported SOFC, as presented in Table 17, are approximately 0.0807%, 0.0545%, and 0.1448%, respectively. Genrally, in this study, electrolyte supported cell generates more uniform temperature profile with minimum temperature difference.

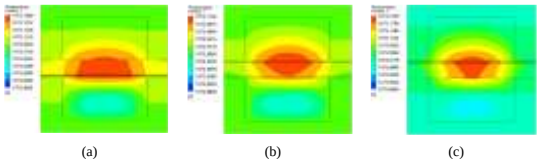

Fig. 2. Temperature distribution at 800°C (1073K). (a) anode-supported SOFC; (b) electrolyte-supported SOFC; (c) cathode-supported SOFC

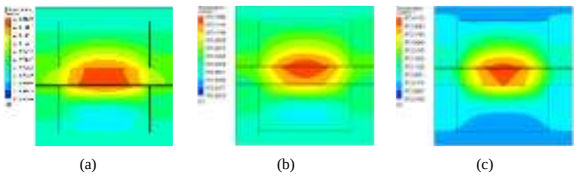

Fig.3. Temperature distribution at 700°C (973K). (a) anode-supported SOFC; (b) electrolyte-supported SOFC; (c) cathode-supported SOFC.

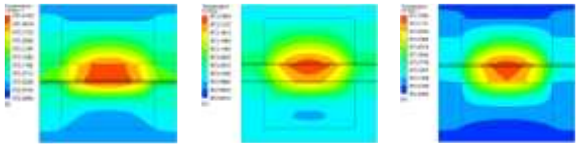

Fig.4. Temperature distribution at 600°C (873K). (a) anode-supported SOFC; (b) electrolyte-supported SOFC; (c) cathode-supported SOFC.

Table 3. Maximum current and power density occurred at 800°C

	SOFC single cell		SOFC interconnect	
	Current density, mA/m²	**Power density, mW/cm²**	**Current density, mA/m²**	**Power density, mW/cm²**
Anode-supported SOFC	4336.1	3035.3	1300.8	910.5
Electrolyte-supported SOFC	1239.4	867.58	371.8	260.2
Cathode-supported SOFC	4467.9	3127.5	1340.4	938.3

Furthermore, the performance of cathode-supported SOFCs with varying anode thicknesses (0.02, 0.03, and 0.04mm) and electrolyte thicknesses (0.01, 0.02, and 0.03 mm) has been compared. Initially, by examining the maximum SOFC power density values at an operating temperature of 800°C, as shown in Table 39, it is evident that reducing the anode thickness from 0.03 to 0.02 mm and the electrolyte thickness from 0.02 to 0.01mm results in an increase in maximum power density from 3127.53 to 3489.22 mW/cm2, representing an approximately 11.56 % power density increase. However, when the anode thickness is increased from 0.03 to 0.04 mm and the electrolyte thickness from 0.02 to 0.03 mm, the maximum power density decreases from

3127.53 to 2251.62 mW/cm2, indicating an approximately 28% reduction in power density.

According to Perng et al. [20], it was reported that as the thickness of the anode layer increases, the distance between the anode inlet and the electrolyte also increases. This leads to greater resistance on the thicker anode side, slowing down fluid flow. This phenomenon can hinder the fuel's movement from the anode to the electrolyte, subsequently reducing cell performance. On the other hand, Chelmehsara and Mahmoudimehr [6] noted that an increase in electrolyte thickness may result in greater difficulty for ions to pass through the thicker electrolyte layer. Therefore, based on the simulation results, it can be concluded that reducing the anode thickness from 0.03 to 0.02mm and the electrolyte thickness from 0.02 to 0.01mm results in higher power generation in a cathode-supported SOFC with a cathode thickness of 0.35 mm

Table 4. Maximum current and power density occurred at 700°C

	SOFC Single cell		**SOFC interconnect**	
	Current density, A/m²	**Power density, mW/cm²**	**Current density, A/m²**	**Power density, mW/cm²**
Anode-supported SOFC	2309.6	1616.7	692.9	485.1
Electrolyte-supported SOFC	882.7	617.9	264.8	185.4
Cathode-supported SOFC	2363.0	1654.1	708.9	496.2

Table 5. Table 3. Maximum current and power density occurred at 600°C

	SOFC Single cell		**SOFC interconnect**	
	Current density, A/m²	**Power density, mA/cm²**	**Current density, A/m²**	**Power density, mW/cm²**
Anode-supported SOFC	1168.6	818.2	3505.7	245.4
Electrolyte-supported SOFC	596.5	417.6	179.5	125.3
Cathode-supported SOFC	1187	830.9	3561	249.3

4 Conclusion

This study analyzes the results of CFD simulations based on various types of supported cells: anode-supported, cathode-supported, and electrolyte-supported SOFCs. The findings reveal that the electrolyte-supported cell exhibits a more uniform temperature distribution, although its power density performance is not notably significant. Conversely, the cathode-supported cell demonstrates the highest power density results with a lower temperature difference. This can be attributed to its larger effective reaction zone and lower cathode ohmic losses. The optimal layer thicknesses identified in this study are as follows: cathode (0.35 mm), anode (0.02 mm), and electrolyte (0.01 mm). In summary, it can be concluded that among the various supported SOFCs, the cathode-supported SOFC performs the best, especially at intermediate operating temperatures. To enhance the cell performance of cathode-supported SOFCs, it is essential to optimize the thickness of the cathode component, as well as the anode and electrolyte. As a recommendation, further research could explore the optimization of the SOFC interconnect rib width, as different rib width designs may yield varying performance outcomes.

The authors thank the Tunku Abdul Rahman University of Management and Technology for supporting this research.

References

1. D. Papurello, S. Silvestri, S. Modena, Biogas trace compounds impact on high-temperature fuel cells short stack performance. Int. J. Hydrogen Energy **46(12)**, 8792-8801 (2021)
2. K.H. Tan, H.A. Rahman, H. Taib, Coating layer and influence of transition metal for ferritic stainless steel interconnector solid oxide fuel cell: A review. Int. J. Hydrogen Energy **44(58)**, 30591-30605 (2019)
3. A. Dhanasekaran, Y. Subramanian, L.A. Omeiza, V. Raj, H.P.H.M. Yassin, M.A. Sa, A.K. Azad, Computational fluid dynamics for protonic ceramic fuel cell stack modeling: a brief review. Energies. **16(1)**, 208 (2022)
4. Ö. Aydın, G. Matsumoto, A. Kubota, D.L. Tran, M. Sakamoto, Y. Shiratori, Performance and durability of one-cell module of biogas-utilizing SOFC equipped with graded indirect internal reformer. J. Electrochem. Soc. **167(6)**, 064512 (2020)
5. A. Iqbal, G. Moskal, Recent development in advance ceramic materials and understanding the mechanisms of thermal barrier coatings degradation. Arch. Comput. Methods Eng. **30**, 4855 (2023)
6. M.E. Chelmehsara, J. Mahmoudimehr, Techno-economic comparison of anode-supported, cathode-supported, and electrolyte-supported SOFCs. Int. J. Hydrogen Energy **43(32)**, 15521-15530 (2018)
7. M. Asmare, M. Ilbas, F.M. Cimen, C. Timurkutluk, S. Onbilgin, Three-dimensional numerical simulation and experimental validation on ammonia and hydrogen fueled micro tubular solid oxide fuel cell performance. Int. J. Hydrogen Energy **47(35)**, 15865-15874 (2022)

8. D. Panuh, S.M. Ali, D. Yulianto, M.F. Shukur, A. Muchtar, Effect of yttrium-stabilized bismuth bilayer electrolyte thickness on the electrochemical performance of anode-supported solid oxide fuel cells. Ceram. Int. **47(5)**, 6310-6317 (2021)
9. H. Shimada, T. Yamaguchi, H. Sumi, Y. Yamaguchi, K. Nomura, Y. Fujishiro, Effect of Ni diffusion into $BaZr_{0.1}Ce_{0.7}Y_{0.1}Yb_{0.1}O_{3-\delta}$ electrolyte during high temperature co-sintering in anode-supported solid oxide fuel cells. Ceram. Int. **44(3)**, 3134-3140 (2018).
10. S. Yang, T. Chen, Y. Wang, Z. Peng, W.G. Wang, Electrochemical analysis of an anode-supported SOFC. Int. J. Electrochem. Sci. **8(2)**, 2330-2344 (2013)
11. A.M. Nassef, A. Fathy, E.T. Sayed, M.A. Abdelkareem, H. Rezk, W.H. Tanveer, A.G. Olabi, Maximizing SOFC performance through optimal parameters identification by modern optimization algorithms. Renew. Energy **138**, 458-464 (2019)
12. N.A.M.N. Aman, A. Muchtar, M.I. Rosli, N.A. Baharuddin, M.R. Somalu, N.S. Kalib, Influence of thermal conductivity on the thermal behavior of intermediate-temperature solid oxide fuel cells. J. Electrochem. Sci. Technol. **11(2)**, 132-139 (2020)
13. K. Yuan, Y. Ji, J.N. Chung, Physics-based modeling of a low-temperature solid oxide fuel cell with consideration of microstructure and interfacial effects. J. Power Sources **194(2)**, 908-919 (2009)
14. R.V. Mangalaraja, S. Ananthakumar, M. Paulraj, H. Pesenti, M. López, C.P. Camurri, L.A. Barcos, R.E. Avila, Electrical and thermal characterization of Sm^{3+} doped ceria electrolytes synthesized by combustion technique. J. Alloys Compd. **510(1)**, 134-140 (2012)
15. A.M. Abdalla, S. Hossain, A.T. Azad, P.M.I. Petra, F. Begum, S.G. Eriksson, A.K. Azad, Nanomaterials for solid oxide fuel cells: A review. Renew. Sustain. Energy Rev. **82**, 353-368 (2018)
16. X. Zhang, M. Espinoza, T. Li, M. Andersson, Parametric study for electrode microstructure influence on SOFC performance. Int. J. Hydrogen Energy **46(75)**, 37440-37459 (2021)
17. S. Su, X. Gao, Q. Zhang, W. Kong, D. Chen, Anode-versus cathode-supported solid oxide fuel cell: Effect of cell design on the stack performance. Int. J. Electrochem. Sci. **10(3)**, 2487-2503 (2015)
18. M. Asmare, M. Ilbas, F.M. Cimen, C. Timurkutluk, S. Onbilgin, Three-dimensional numerical simulation and experimental validation on ammonia and hydrogen fueled micro tubular solid oxide fuel cell performance. Int. J. Hydrogen Energy **47(35)**, 15865-15874 (2022)
19. R.V. Kumar, A.P. Khandale, A review on recent progress and selection of cobalt-based cathode materials for low temperature-solid oxide fuel cells. Renew. Sustain. Energy Rev. **156**, 111985 (2022)
20. S.W. Perng, C.R. Chen, Numerical investigation of anode thickness on the performance and heat/mass transport phenomenon for an anode-supported SOFC button cell. J. Nanomater. **16(1)**, 197-197 (2015)